

TeAAL: A Declarative Framework for Modeling Sparse Tensor Accelerators

Nandeeka Nayak*, Toluwanimi O. Odemuyiwa**, Shubham Ugare*, Christopher W. Fletcher*, Michael Pellauer†, Joel S. Emer†‡

*University of Illinois–Urbana Champaign, **University of California–Davis, †NVIDIA, ‡Massachusetts Institute of Technology
{ndnayak2, sugare2, cwfletch}@illinois.edu, todemuyiwa@ucdavis.edu, mpellauer@nvidia.com, jsemer@mit.edu

ABSTRACT

Over the past few years, the explosion in sparse tensor algebra workloads has led to a corresponding rise in domain-specific accelerators to service them. Due to the irregularity present in sparse tensors, these accelerators employ a wide variety of novel solutions to achieve good performance. At the same time, prior work on design-flexible sparse accelerator modeling does not express this full range of design features, making it difficult to understand the impact of each design choice and compare or extend the state-of-the-art.

To address this, we propose TeAAL: a language and compiler for the concise and precise specification and evaluation of sparse tensor algebra architectures. We use TeAAL to represent and evaluate four disparate state-of-the-art accelerators—ExTensor, Gamma, OuterSPACE, and SIGMA—and verify that it reproduces their performance with high accuracy. Finally, we demonstrate the potential of TeAAL as a tool for designing new accelerators by showing how it can be used to speed up Graphicionado—by $38\times$ on BFS and $4.3\times$ on SSSP.

1. INTRODUCTION

Sparse tensor algebra workloads have exploded in popularity over the past few years, with applications ranging from deep learning [4, 23, 42] to graph algorithms [3, 5, 10, 24, 28, 38] to physical simulations [18, 43, 44]. This surge has been accompanied by a corresponding rise in proposals for custom hardware to service common sparse kernels, e.g., sparse matrix multiply [13, 14, 31, 33, 35, 48, 49]. While these accelerators have the potential to provide dramatic speedup over the best CPU and GPU algorithms, they take significant effort and space to describe, refine, and evaluate. Specifically, accelerators are typically described with RTL or a block diagram and accompanying natural language description. The former is verbose and often difficult to comprehend, while the latter is imprecise and often incomplete. Neither make it easy to model and evaluate the impact of proposed design changes.

In contrast, for *dense* tensor accelerators, a number of tools support concise, precise specifications and the derivation of efficient models [21, 32, 47]. To simplify specification [36], these tools support separately providing a target *algorithm* (i.e., a functional description of the problem, such as an equation in Einstein summation (Einsum) notation [11]) and a *mapping*, expressing when and where in the processor each action (e.g., compute or storage access) occurs [7]. These, together, correspond to a *mapped representation* (e.g., a loop nest), describing both the algorithm and how it is executed. A *model of the target platform* then evaluates the mapped rep-

resentation to produce metrics like performance and energy.

The goal of this work is to extend the above level of tool support to accelerators working on sparse tensors. Modeling sparse tensor kernels is challenging for several reasons:

First, tools targeting dense tensor algebra cannot accurately model the work performed by sparse tensor kernels. These tools model workloads analytically, using a few summary statistics (like tensor shapes) to accurately capture the characteristics of dense tensors, and therefore dense kernels. However, such summary statistics cannot capture the variety in sparsity distributions present in real-world tensors.

Second, unlike in the dense case, non-uniform, input-dependent sparsity necessitates specialized algorithms and mechanisms to cope with irregular (often low) data reuse, myriad compression formats, additional meta-computation (e.g., intersection), and more. For example, the OuterSPACE accelerator [31] splits sparse-sparse matrix multiply (SpM-SpM) into several phases that respectively produce, sort, and consume an array of linked lists representing partial products. Gamma [48] executes the same kernel with Gustavson’s algorithm and using a high-radix hardware merger to do so efficiently. SIGMA [35] uses yet a third strategy (irregularly filling a PE array with only non-zero data). And so on.

Unfortunately, existing tools for modeling sparse tensor algebra accelerators do not fully overcome these challenges. For example, STONNE [26, 27] supports only the monolithic SpMSpM kernel, and even then, only six pre-selected mappings for said kernel. Sparseloop [46] can model an accelerator describable in a single deep loop nest. As we will show, this is insufficient to express SIGMA, OuterSPACE, and Gamma. Additionally, Sparseloop uses abstract distribution functions to model sparsity, rather than precisely modeling the behavior of actual input sets. While better than using *just* shape-based information (like dense modeling), we show how this approach still results in degraded modeling accuracy (Section 7).

This work. We address the above challenges by showing how recent sparse tensor algebra accelerators can be expressed as cascades (DAGs) of mapped Einsums and *content-preserving transformations* on the constituent tensors in said Einsums. For example, both OuterSPACE and Gamma can be described by rewriting the Einsum for matrix multiply into several, dependent Einsums. In this abstraction, the sort/merge operations in said designs are described as *reordering the dimensions* of an intermediate tensor to improve locality, while the differences between the two operations are captured in how each Einsum is mapped. We show how the major activities in other accelerators can likewise be described in terms of a small set of similar operations, e.g., splitting/combining

dimensions of a tensor while preserving its contents.

Based on the above abstraction, we propose TeAAL (for *Sparse Tensor Algebra Accelerator Language*), a novel declarative language and compiler that enables precise design specification and modeling of sparse tensor algebra accelerators. The TeAAL compiler takes accelerators described as mapped Einsum cascades and produces an imperative-style IR that describes tensor transformations as primitive operations on *fibertrees* [42] (Section 2.1). It then uses implementation-level specifications (e.g., describing the tensor formats) to augment the IR to produce an accurate, validated performance model that processes real sparse tensors.

Although attributes such as language expressivity and conciseness are difficult to quantify, as part of a study to validate TeAAL’s fidelity, we write the TeAAL Einsum and mapping specifications of four recent (and disparate) sparse tensor algebra accelerator proposals (OuterSPACE [31], ExTensor [14], Gamma [48], and SIGMA [35]) in less than a page (see Figures 3 and 7), with each specification taking ~ 30 lines. We verify that the models generated for each of these accelerators reproduce the designs’ original published performance results (given the same input data sets) with high accuracy.

We also show how TeAAL can be applied in adjacent domains and be used to explore optimization opportunities for accelerators in said domains. Specifically, we use TeAAL to describe Graphicianado [12], which accelerates vertex-centric programming (a popular paradigm for solving graph problems), and demonstrate how one can improve Graphicianado by making point changes to its TeAAL specification.

Popping up, TeAAL fills two crucial niches in the field of sparse tensor algebra accelerator design. First, it allows architects to precisely compare more complex designs than current tools in an apples-to-apples fashion and understand the pros and cons of each. Furthermore, it allows architects to efficiently evaluate and iterate on accelerator designs.

To summarize, we make the following contributions:

- We show how modern sparse tensor accelerator features can be represented using cascades of mapped Einsums and content-preserving transformations on those Einsums’ constituent tensors. Based on this abstraction, we propose the TeAAL specification language for concisely and accurately specifying the architecture of sparse tensor algebra accelerators.
- We propose and design a compiler for transforming TeAAL specifications into an imperative-style IR that performs operations on fibertrees and lowering said IR to an accurate performance model of the specified architecture that processes real sparse tensor inputs.
- We validate TeAAL’s accuracy in terms of modeling memory traffic, performance, and energy with respect to the reported results of four state-of-the-art accelerators.
- We demonstrate the potential of TeAAL as a tool for accelerator design by showing how it can be used to speed up Graphicianado [12]—by $38\times$ on BFS and $4.3\times$ on SSSP.

If accepted, we plan to make TeAAL open source.

2. BACKGROUND AND MOTIVATION

We review key attributes of sparse tensor algebra and outline the design decisions typically made by sparse tensor

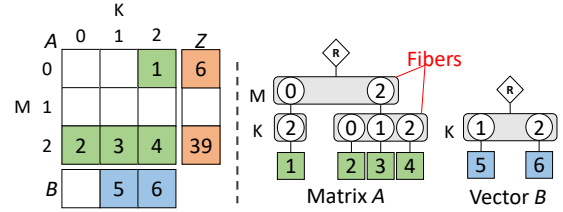


Figure 1: Sparse matrix-vector multiplication and corresponding fibertree representations.

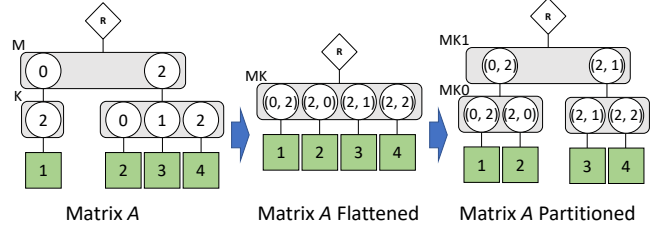


Figure 2: Flattening then partitioning ranks M, K of tensor A (Fig. 1).

accelerators. We highlight the difficulties with informal comparisons between accelerators and motivate the need for a precise, formal specification.

2.1 Tensors and Fibertrees

In this paper, an N -tensor is a multidimensional array with N dimensions. For example, a 0-tensor is a scalar, a 1-tensor is a vector, and a 2-tensor is a matrix. Figure 1 shows a 2-tensor, A , with dimensions M and K . Using the terminology from Sze et al. [42] we describe a tensor’s attributes:

- A *rank* refers to an axis/dimension in the tensor. A matrix has two ranks, often described as rows and columns.
- A *point* is a logical location within a tensor that contains a scalar *value*. A point is identified by an N -tuple of *coordinates* with one for each rank in the tensor. We denote the tensor A ’s element at point (m, k) as $A_{m,k}$.

Mathematically, tensors have no notion of sparsity or compression format. To avoid getting bogged down in the numerous details of various formats, we leverage the following abstractions proposed in Sze et al. [42]:

- A *fibertree* represents a tensor as a tree, with each level corresponding to a labeled rank in the tensor. Tensor A in Figure 1 has ranks M and K .
- The order of levels a fibertree reflects is its *rank order*, denoted $[M, K]$, and read top-to-bottom in the tree.
- Every level contains one or more *fibers*. A *fiber* is the set of elements sharing all coordinates in all higher levels of the tree. Fibers are more precise than “rows” or “columns,” because they naturally extend to N -tensors.
- Each *element* in the fiber is a coordinate/payload pair, where the *payload* is a scalar value when it is at a leaf or a reference to a fiber when it is an intermediate node.
- A tensor’s *shape* is the maximum number of elements each fiber in each rank can contain. For example, tensor A in Figure 1 has shape $M \times K$, where $M = K = 3$.

One advantage of fibertrees is that they naturally handle both dense and sparse tensors (i.e., tensors where a number of points are zero). A dense tensor’s fibertree has every coordinate present in the entire shape (i.e., a complete tree).

On the other hand, a sparse tensor’s fibertree can omit all elements with empty payloads (either zero values or empty fibers). The semantics of operations on fibers and fibertrees remain the same in both cases. Note that fibertrees are just an abstraction we use to describe operations on tensors. To model a specific design, all fibertrees are lowered to concrete representations, like CSR or COO (see Section 4.1.1).

This abstraction also supports a number of transformations that change the fibertree corresponding to a tensor, but do not modify the underlying tensor:

- A *rank flattening*, demonstrated in the first transformation in Figure 2, combines two ranks together into a single rank. After flattening, the coordinates are tuples of the coordinates in the original fibers that reference a payload from the original lower rank.
- A *rank partitioning*, demonstrated in the second transformation in Figure 2, separates a rank into two ranks. The coordinates of the new upper rank denote the first valid coordinate in the fiber below.
- A *rank swizzle* changes the fibertree’s rank order (i.e., reorders the levels of the fibertree).

As we will see in Section 3, many of the ways that hardware accelerators modify their tensors to improve efficiency can be viewed as one or more of these transformations.

2.2 Tensor Algebra with Einsums

For this work, we present an operational definition of an extended Einsum, which specifies the individual computations to occur [11, 14, 42]. Einsums have been used as the tensor algorithm specification in prior work for tensor algebra compilation [20] and accelerator modeling [32, 46]. An Einsum specifies three things: (1) the input and output tensors involved and their ranks, (2) an *iteration space* relating the ranks together as well as the limits of that space, and (3) the computation to be performed at each point in the space. For example, the Einsum for matrix-vector multiply is:

$$Z_m = A_{m,k} \times B_k. \quad (1)$$

Here, the iteration space—the Cartesian product of all legal coordinates in the expression—is $M \times K$. An implementation of this Einsum must traverse each point in this space. For each point, it computes the operation (\times) on the right-hand-side using the specified points in the input operands (A, B). It then takes the result and populates the location specified in the left-hand-side (Z). Since the K rank does not appear in the output tensor, the Einsum will attempt to repeatedly populate the same point (Z_m). Einsum semantics resolve this by reducing the multiple values—e.g., using $\sum_{k=0}^K$ —to a single value for that point. Note that the Einsum does not specify iteration order; this is left to mapping (Section 2.3).

By adding a new rank N to B , we can extend the Einsum to matrix multiplication:

$$Z_{m,n} = A_{m,k} \times B_{k,n}. \quad (2)$$

This expands the iteration space to $M \times K \times N$.

2.3 Mapping Hardware Accelerators

Mapping [7] is the task of scheduling the computation of an Einsum onto limited hardware resources to jointly optimize for the desired combination of throughput, latency (execution

time), power, etc. We summarize the mapping attributes used for hardware modeling and design in prior work [6, 15, 17, 21, 25, 32, 47] that we use throughout.

1) Loop order. The Einsum’s large iteration space must be serialized through finite datapath resources in some order. Two choices for Equation 1 are: (1) $[M, K]$ or (2) $[K, M]$. Loop order is read left-to-right, topmost-to-bottommost loop. For example, (1) above reads “for each value of m , iterate through all values of k .” This choice affects data locality and, in turn, memory access costs. Depending on on-chip buffer sizes, loop order (1) for matrix-vector multiply keeps an element of Z *stationary* [7] in on-chip memory while B is streamed in multiple times. Meanwhile, loop order (2) keeps B stationary but repeatedly streams Z .

2) Splitting. To further improve data locality across all tensors, many algorithms employ splitting (or strip mining, blocking, etc.) to divide the iteration space into subspaces that refer to a small enough subset of each of the tensors that they fit fully in on-chip buffers. Fibertrees model these subsets by partitioning their fibers according to the split iteration space. How a fiber is partitioned is a function of the coordinates in the fiber. For example, suppose matrix A has a rank-order of $[M, K]$. Splitting K by shape $K0$ results in a new A tensor with rank-order $[M, K1, K0]$, where K is split into $K1$ partitions with $K0$ coordinates each.¹

3) Work scheduling. Finally, the mapping specifies how the iteration space is traversed, by placing each point at a specific location in both time and space. Mapping a computation at different locations in time implies that the computation is serial (i.e., computations happen one after another on the same component), while mapping at different locations in space implies parallelism (i.e., computation happens at the same time on different processing elements (PEs)).

2.4 Accelerating Sparse Tensor Algebra

Sparse tensor algebra introduces new opportunities and challenges to the mapping problem. Sparse tensors are typically *compressed* to remove the zero elements, resulting in fibertrees with missing coordinate-payload pairs. Compression can yield significant savings in storage and data transfers and avoid ineffectual compute—operations that have no impact on the result and can be safely skipped, e.g., multiplication or addition with zero [14].

However, realizing these benefits requires accelerators to “sparsify” the iteration space, or remove the ineffectual compute, increasing design complexity, sensitivity to memory latency/bandwidth, and load imbalance. For example, the $[M, K]$ loop order for Equation 1 may move, for example, from $(m=0, k=2)$ to $(m=2, k=0)$ in one step. Sparse tensors also require *co-iteration* of the operands and additional operations (e.g., intersection for fibers multiplied together) to remove ineffectual compute. Without careful engineering, this can lead to inefficiencies that do not occur when tensors are dense [29]. For example, the same-shape tiles produced by the scheme described in Section 2.3 may have different memory footprints, leading to data transfer and compute load imbalance when tiles are distributed to workers.

To deal with these challenges, sparse tensor accelerators

¹In other words, each tile stores coordinates in the coordinate range $[i * K0, (i + 1) * K0]$ for some i .

Table 1: Comparison of selected sparse tensor accelerator hardware proposals. TeAAL specifications increase both the precision and formalism of such comparisons, and enable automatic generation of performance/energy models.

Accelerator	Year	Mapping Approach	Architectural Focus
OuterSPACE [31]	2018	Outer Product parallelized across rows of A	Sparse matrix multiply with serial multiply/add phases, custom merge unit
ExTensor [14]	2019	Inner Product tiled across all dimensions for locality	Arbitrary Einsums and TACO formats [8], skip-ahead intersection unit
MatRaptor [39]	2020	Row-wise Product with parallel summation	Sparse matrix multiply with co-design of micro-architecture and C ² SR format
SIGMA [35]	2020	Inner Product parallelized across multiple dimensions	Sparse matrix multiply with custom bitmap format, flexible hardware topology
SpArch [49]	2020	Outer Product with parallel merge	Sparse matrix multiply with optimized RAM interface in sum phase
Tensaurus [40]	2020	Inner Product with extended scalar-fiber product followed by fiber-fiber product (SF^3)	SF^3 demonstrated applicability to multiple Einsums beyond matrix-matrix multiply
Gamma [48]	2021	Row-wise Product, adoption of Gustavson’s alg.	Sparse matrix multiply with custom FiberCache, transposed merge-and-sum

have proposed a wide variety of custom hardware solutions, summarized in Table 1. We note that the complexity of this topic makes such a table an imprecise and ultimately unsatisfying comparison. Additionally, all of these works used custom hand-written simulators of actual data sets to ensure all complexities are captured. In the remainder of this paper we present a formalism to resolve this imprecision and enable concise apples-to-apples comparison. TeAAL supports the automatic generation of performance/energy models for a wide range of accelerators, significantly reducing engineering effort during design-space search. We think that this approach is extensible, and TeAAL can easily be modified to support new accelerator features.

3. OVERVIEW AND INSIGHTS

We now propose TeAAL: a language and compiler that 1) enables the concise specification of a sparse tensor algebra accelerator and 2) generates efficiency statistics for that accelerator computing on actual sparse tensors.

Our key conceptual contribution, which guides the design of TeAAL, is to show that recent sparse tensor algebra accelerators can be expressed as directed, acyclic graphs (DAGs or *cascades*) of mapped Einsums (Sections 2.2, 2.3) and content-preserving transformations on their tensors. We show how these transformations, along with the computations done within each Einsum, can be expressed as a small set of primitive operations on fibertrees (Section 2.1). This can be articulated as two novel insights:

Insight 1: Einsum cascades can represent multi-phase accelerator designs (Section 3.1). We show that cascades of Einsums are sufficiently expressive to represent computations broken into multiple disparate phases (e.g., Toeplitz-based convolution, OuterSPACE’s multiply-merge and Graphicionado’s process and apply).

Insight 2: Fibertree operations can represent the content-preserving transformations applied to mapped tensors (Section 3.2). By abstracting tensors as fibertrees, we reduce a range of tensor transformations into a few core operations. We use fibertree rank partitioning/flattening as a general pattern for representing both sparse tensor splitting and work scheduling strategies. We also show how fibertree rank swizzling improves tensor traversal efficiency and manifests as a variety of sorting mechanisms (e.g., the insertion sort in OuterSPACE and the high-radix hardware merger in Gamma).

This section describes the above insights in more detail, and how they enable the design of the TeAAL specification language. Section 4 describes how the TeAAL compiler converts said specifications into an imperative-style IR de-

scribing operations on fibertrees, and how this IR (augmented with some additional information, e.g., describing the architecture and concrete formats) is subsequently converted into an accurate performance model.

TeAAL specifications. The TeAAL *specification language* is a declarative, domain-specific language (DSL) that defines the computation as a cascade of Einsums (*expressions*), attributes on each tensor (*declaration, rank-order, partitioning*), and a dataflow that describes when and where those tensors’ data is moved (*loop-order, spacetime*). Rank swizzling is not shown explicitly, but is inferred from other mapping attributes, such as the *rank-order* and *loop-order*.

OuterSPACE running example. Throughout this section and Section 4, we use the example TeAAL specification in Figure 3, which describes the OuterSPACE accelerator [31]. At a high level, OuterSPACE accelerates SpMSpM using the *multiply-merge* algorithm. It first performs all multiplications between input tensors A and B in an outer-product fashion, writes resulting partial products to an array-of-linked-lists data structure, sorts the linked lists to facilitate reduction, and finally performs said reductions to derive final results. We now discuss how TeAAL both implicitly and explicitly captures the key components of OuterSPACE.

3.1 Insight 1: Einsum cascades capture multi-phase accelerators

Our first insight is that seemingly monolithic tensor algebra kernels (e.g., matrix multiply) are often implemented as a DAG of operations, and that each of these operations can be expressed as an Einsum that produces and consumes intermediate tensors. We call this DAG a *cascade*. For example, consider a 1D convolution between input I and filter F . Convolution is performed using two predominant implementation styles. The first style is direct convolution, which is often employed by accelerators. As an Einsum, direct convolution is written as

$$O_q = I_{q+s} \times F_s \quad (3)$$

An alternative style is the Toeplitz expansion [42], which converts the convolution into a matrix-vector or matrix-matrix multiply and is common on systolic arrays and data-parallel processors like GPUs. First, the input is refactored into a matrix to enable, in this case, matrix-vector multiplication between the input (now stored in T) and the filter F in the second stage. An important observation is that this can be written as the following sequence of dependent Einsums:

$$T_{q,s} = I_{q+s}; \quad O_q = T_{q,s} \times F_s \quad (4)$$

Importantly, the RHS of the Einsum used to generate T mirrors how I is indexed in the Einsum for direct convolution.

```

1 einsum:
2   declaration : # Ranks are listed alphabetically in this section.
3   A: [K, M]    # Rank order is specified below in rank-order.
4   B: [K, N]
5   T: [K, M, N]
6   Z: [M, N]
7   expressions :
8     - T[k, m, n] = A[k, m] * B[k, n] #  $T_{k,m,n} = A_{k,m} \times B_{k,n}$ 
9     - Z[m, n] = T[k, m, n] #  $Z_{m,n} = T_{k,m,n}$ 
10  mapping:
11    rank-order:
12      A: [K, M]
13      B: [K, N]
14      T: [M, K, N]
15      Z: [M, N]
16    partitioning :
17      T:
18        M: [uniform_occupancy(A.256), uniform_occupancy(A.16)]
19      Z:
20        M: [uniform_occupancy(T.128), uniform_occupancy(T.8)]
21    loop-order:
22      T: [K, M2, M1, M0, N]
23      Z: [M2, M1, M0, N, K]
24    spacetime:
25      T:
26        space: [M1, M0]
27        time: [K, M2, N]
28      Z:
29        space: [M1, M0]
30        time: [M2, N, K]

```

Figure 3: TeAAL specification for the Einsums and mappings of OuterSPACE [31], described in detail in Figure 3.

The Toeplitz expansion simply relaxes the requirement that the access into I and the corresponding access into F happen at the same time. Decomposing an Einsum into a cascade enables each resulting Einsum to be mapped independently, exposing new degrees of freedom for building and using intermediate tensors. Note that this sequence of Einsums says nothing about how (if at all) the two stages are overlapped. They can happen entirely sequentially, or the accelerator can implement pipeline parallelism. For example, the Q rank can be partitioned (Section 3.2.1) and once a partition of T is produced, it can be consumed by the multiply stage. Section 4.3 describes how TeAAL determines this parallelism.

Beyond convolution, cascades of Einsums can be used to represent other common implementation styles in sparse tensor algebra accelerators. For example, they capture the multiply-merge algorithm in the OuterSPACE example (Figure 3). During the multiply phase (Line 8), columns of the A matrix are multiplied with rows of the B matrix to form partial products, which we call T . Then, during the merge phase, specified by the second Einsum (Line 9), T is reduced along the K rank, yielding the final result Z .

Sparsity also motivates new operations on tensors, and our Einsum notation can be extended to include them if needed. We currently support one—the `take(.)` operator—which decouples intersection from computation with the following semantics: if at least one of the inputs is zero at a point, the output is zero, otherwise, copy one of the inputs into the output. Take the example:

$$T_{k,m,n} = \text{take}(A_{k,m}, B_{k,n}, 1)$$

The final parameter denotes which input is copied into the output. This example copies B into T , but if the last parameter were 0, A would be copied.

3.2 Insight 2: Fibertree operations can represent the content-preserving transformations applied to mapped tensors

Our second insight is that, by abstracting tensors as fibertrees, we can reduce a range of tensor transformations into a few core operations. Fibertree rank partitioning (and its inverse: flattening) can be used as a single abstraction for specifying both sparse tensor splitting and work scheduling strategies. Similarly, transposing data in memory, sorting, and merging are all tantamount to fibertree rank swizzling.

3.2.1 Sparse Tensor Splitting and Work Scheduling

Recall from Section 2.3 that splitting for dense problems is shape-based. This can be expressed by partitioning a fibertree rank at coordinate-based boundaries given by the tile dimension. Unfortunately, when data is sparse, this strategy can lead to low reuse and under-utilization of tiles (and therefore buffers) [29], i.e., if different partitions have different occupancies. A key observation is that partitioning naturally generalizes to other types of splitting that *can* adapt to irregular sparsity, simply by changing the *partitioning criteria*, i.e., where the partition boundaries occur. From studying existing accelerators, we define a simple sparsity-aware strategy we call *uniform occupancy-based partitioning*. In this scheme, each fiber at a level in the fibertree is split so that each new fiber has an equal number of elements (modulo remainders). Importantly, each fiber’s coordinate range after an occupancy-based partitioning is irregular. Thus, to ensure that partitions of multiple tensors have matching coordinate ranges for co-iteration (Section 2.4), occupancy-based partitioning uses a *leader-follower* paradigm: the partitions’ coordinate ranges are chosen so that the leader tensor’s partitions are equal occupancy and all follower tensors adopt those ranges.

More subtly, we observe that partitioning is also a useful abstraction through which to specify work scheduling when work is parallelized. Consider OuterSPACE, which works on 256 non-empty elements of matrix A at a time during the multiply phase, further subdividing these into 16 groups of 16 elements to each be processed by a “Processing Tile” (a group of PEs [31]). The TeAAL specification for OuterSPACE (Figure 3) represents these on Line 18 as occupancy-based partitioning applied twice hierarchically, with the A tensor serving as the leader.² The TeAAL specification describes the parallelism this partitioning enables on Line 26 by scheduling ranks $M1$ and $M0$ in space (Section 2.3).

Unfortunately, occupancy-based partitioning may result in partitions with uneven data footprints because a partition must end where its parent fiber ends. Flattening (Section 2.1), when combined with occupancy-based partitioning, mitigates this imbalance by first combining all ranks, then redistributing the elements so that, globally, each partition has the same number of values. For example, Figure 2 shows how a fibertree whose fibers start with an unequal number of coordinates can be flattened and re-partitioned to equalize the number of coordinates per partition. Note that, though all partitioning directives modify the fibertree abstract representation, the concrete representation may remain unchanged.

²Note: OuterSPACE only enables half its PEs during the merge step, so the occupancy-based partitioning applied to the second Einsum (Line 20) only involves 128 PEs (8 per “Processing Tile”).

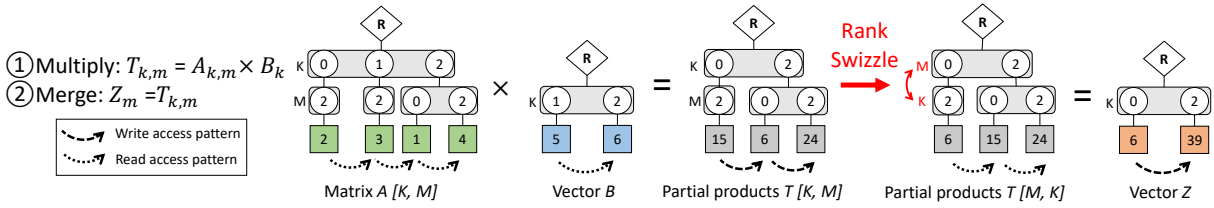


Figure 4: Rank swizzling in sparse tensor algebra computations, using outer-product multiply-merge matrix-vector multiplication. Matrix A and vector B use values from Figure 1 for consistency. An offline rank swap ensures that A has rank order $[K, M]$ prior to the multiply phase, and an online rank swap ensures that T has rank order $[M, K]$ prior to the merge phase, ensuring concordant traversal in both phases.

3.2.2 Transposition, Sorting, and Merging

We observe that tensor algebra computations often perform operations that, when expressing their tensors in the fibertree abstraction, are tantamount to fibertree rank swizzles. These operations enable the more efficient *concordant* (as opposed to *discordant*) traversal [42]. Concordant traversal occurs when a loop nest traverses a fibertree in the order in which its ranks appear, i.e., traverses each fiber sequentially and in a depth-first manner. For example, matrices A and B in Figure 3 are traversed concordantly. K is the top-most rank in both the rank and loop orders for the multiply stage (Lines 12-13, 22), and $M2$, $M1$, $M0$, and N appear below. Thus, we never have to search for the next $m2$, $m1$, $m0$, or n coordinate, it is always either the first or next coordinate in the current fiber(s).³ Conversely, iterating over K in the bottom-most loop would be a discordant traversal (for this rank order).

It is common practice to swizzle ranks to enable concordant traversal on input tensors. For example, the transposition of a matrix from the CSR format into the CSC format can be viewed as a rank swizzle, and is used by OuterSPACE to achieve a $[K, M]$ rank order on A (Line 12) in preparation for the outer-product-style multiply phase. Input tensor swizzles are usually performed offline. More subtly, we observe that sparse tensor accelerators also perform rank swizzles on *intermediate tensors* formed during kernels expressed as cascades of Einsums (Section 3.1). Depending on whether coordinates in the intermediate tensors are stored in sorted or unsorted order and on the extent to which the intermediate tensors are built before being consumed, this either requires a merge or a (more expensive) sort operation.

Figure 4 shows an example of a multiply-merge for outer product, matrix-vector multiplication. To support concordant traversal on both input and output tensors, the multiply phase uses a $[K, M]$ loop order, while the merge phase uses an $[M, K]$ loop order. Thus, at the end of the multiply phase, T has rank order $[K, M]$. Then, during the reduction, a rank swap changes the rank order of T to $[M, K]$ to match the $[M, K]$ loop order. The dashed arrows in Figure 4 show that *both* the tensor read and write access patterns through A , B , T , and Z are all concordant through both phases. Importantly, such online rank swaps may degrade performance, and therefore warrant dedicated hardware support. Yet, they can significantly improve spatial/temporal locality, and thus, appear in multiple prior designs [31, 48, 49].

By default, TeAAL infers rank swizzling automatically to

³Though sequential iteration through a fiber is efficient in many concrete representations, it can be very inefficient. The true cost of iteration is accounted for during modeling (Section 4).

Table 2: Supported hardware components and their attributes.

Component	Attributes
DRAM	bandwidth
Buffer	type (buffer [34] or cache), width, depth, bandwidth
Intersection	type (two-finger, leader-follower, or skip-ahead), leader
Merger	inputs, comparator_radix, outputs, order (fifo, opt), reduce
Compute	type (mul or add)

maintain concordant traversal. For example, for OuterSPACE (Figure 3), T has rank order $[M, K, N]$, but TeAAL produces T during the multiply phase in $[K, M, N]$ order, swizzles it to $[M, K, N]$ order to be stored in memory, and then swizzles it again to $[M, N, K]$ order to prepare for the merge.

4. GENERATING THE MODEL

In Section 3, we showed that the fibertree abstraction is general enough to describe many of the design decisions used in sparse tensor accelerators. However, to manifest a specific design, the fibertrees must be lowered onto concrete representations and their operations bound to specific hardware components. In this section, we define three additional specifications—*format*, *architecture*, and *binding*—used by TeAAL to perform this lowering, and describe how these plus the *einsum* and *mapping* specifications from Section 3 are combined to produce an executable model for evaluating accelerator workload performance.

4.1 Lowering Mapped Einsums to Hardware

This section describes three additional specifications, the *format*, *architecture*, and *binding*, that are used to lower mapped Einsums to concrete representations and hardware resources.

4.1.1 Format

Prior works on modeling sparse tensor algebra computations [8, 42, 46] propose a convenient abstraction for translating a fibertree to the actual data footprint: a per-fiber format. However, the formats used by existing sparse accelerator modeling frameworks restrict themselves to a fixed number of common configurations (e.g., bitmap [27] or uncompressed offset pointers [46]).

TeAAL enables more modular specification, capturing a larger class of formats than existing tools, by separating the attributes of a fiber’s format into three categories: a format type, a layout, and data widths for the coordinates, payloads, and fiber headers. Fibers are concretized as an array of coordinates and a array of payloads (struct-of-arrays) or as a single array of elements (array-of-structs). TeAAL supports three

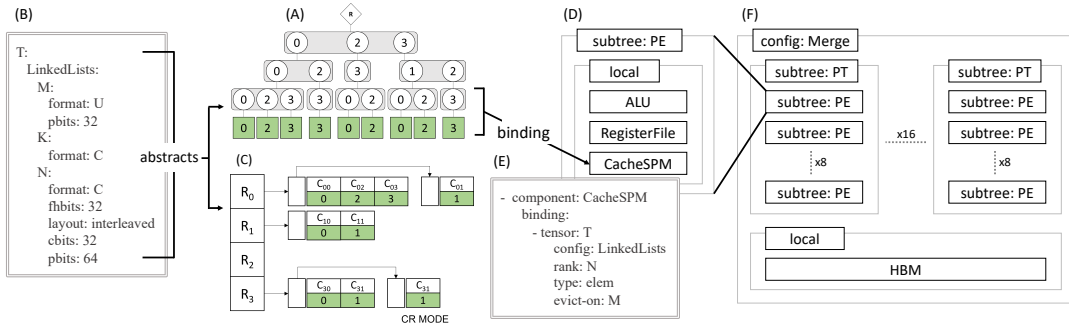


Figure 5: TeAAL concrete/hardware-level model of the OuterSPACE accelerator [31]. The fibertree (A) combined with the format specification (B) describe the concrete representation, a custom array-of-linked-lists format (C). TeAAL specifies the architecture hierarchically (F), where each level has a set of local components (D) that have tensor operations bound to them (E).

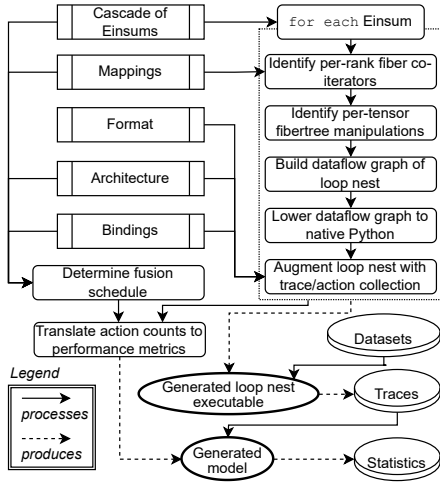


Figure 6: TeAAL tool flow diagram, described in detail in Section 4.3.

format types: uncompressed (U)—where the sizes of the data arrays correspond to the shape of the fiber, compressed (C)—where the sizes of the data arrays correspond to the occupancy of the fiber, or a combination (B)—where the coordinates are uncompressed and the payloads are compressed. For simplicity, currently, all fibers in a rank have the same format. Note that not all information in the fibertree is stored explicitly, e.g., an uncompressed fiber does not need to store coordinates because they can be inferred from the position of the payloads. TeAAL supports this by allowing the corresponding data width—in this case, *cbits*—to be unspecified or set to 0.

This specification is flexible enough to support a variety of common formats (e.g., dense arrays and CSR) and custom formats (e.g., from OuterSPACE [31] and SIGMA [35]). TeAAL also supports multiple formats for the same tensor (differentiated by the configuration name), since manipulating the fibertree may cause the representation to change dynamically.

4.1.2 Architecture

The TeAAL architecture specification (inspired by Time-loop [32]) describes the accelerator topology as a tree of compute and storage units. At each level of the hierarchy, one can define a list of hardware components local to that

level and a list of subtrees below that level. In addition to the component classes supported by Timeloop, we define new classes of components that are involved in performance-limiting operations on sparse accelerators, including caches, intersection units, and hardware mergers. Table 2 gives the full list of supported classes and their attributes. Since an accelerator (e.g., OuterSPACE [31]) may reorganize itself during the execution of a single computation, TeAAL also supports specifying multiple topologies for the same design.

4.1.3 Binding

Finally, TeAAL’s binding specification matches the Einsum- and mapping-induced fibertree operations to specific concrete representations and hardware components. First, each Einsum must be bound to a single accelerator topology. Then, for each storage component, the binding describes what data resides there—as specified by its tensor, configuration, rank, and type (e.g., payload)—and sometimes (e.g., for buffers [34]), for how long. Similarly, for each compute component, the binding describes which compute operations are performed on that component.

4.2 Specifying OuterSPACE [31]

We continue to use OuterSPACE as a running example to motivate the features provided by TeAAL. Figure 5 shows a simplified version of OuterSPACE’s custom tensor format, its architecture during the merge phase, and the correspondence between the fibertree representation of T and its concrete representation and binding. In Figure 5A, we see the fibertree for an example tensor T . The format specification (Figure 5B) for this tensor lowers it onto OuterSPACE’s custom array-of-linked-lists format (Figure 5C). To differentiate it from other representations of the same tensor, we give it the configuration name *LinkedLists*. On the M rank, the array of pointers is given by an uncompressed (U) array of payloads. On the N rank, the fiber header data width (*fhbits*) describes the linked list pointers, the *layout* describes that corresponding coordinates and payloads are adjacent (array-of-structs), and the *cbits* and *pbits* describe the data widths of the coordinates and payloads, respectively.

Figure 5D shows an OuterSPACE PE. During the merge phase, this level has three components: the ALU, the register file, and the L0 scratchpad. OuterSPACE loads the entire subtree under a given M coordinate into the L0 scratchpad

to perform its sort. TeAAL expresses this binding with the specification given in Figure 5E. The *tensor*, *config*, *rank*, and *type* denote exactly what data is buffered, and the *evict-on* keyword is required for binding to explicitly managed buffers, whose fill and drain policy must be set by the user. Because the elements bound to this buffer evict on M , old data is drained when the M coordinate changes. Finally, Figure 5F shows an overview of the entire accelerator topology.

4.3 Compiler and Model Operation

Figure 6 demonstrates how TeAAL puts everything together. For each Einsum in the cascade, TeAAL combines the equation with its mapping information to identify the necessary per-tensor fibertree manipulations (e.g., rank swizzling) and per-rank fiber co-iterators (e.g., intersection). Using this information, it builds a dataflow graph of a loop nest, which it then lowers to an embedded, domain-specific language within Python for executing computations as fibertree operations [1]. The resulting code is an imperative-style representation of the Einsum cascade (i.e., a series of loop nests, one per Einsum), which can directly evaluate real tensors represented as fibertrees.

TeAAL breaks the modeling of an accelerator into two stages. First, the loop nests perform the computation on fibertrees (storing real tensor data) and generate a trace of when each coordinate and each payload is accessed. Then, a model processes those traces to generate statistics that describe the accelerator’s performance characteristics. In this work, we compute statistics with a bottleneck analysis. We identify five crucial bottlenecks in sparse tensor algebra accelerator performance: multiplication, addition, intersection, rank swizzling, and data movement. The model tallies individual operations for each component (e.g., cache hits and misses, intersection tests, etc.), and then computes the performance of each Einsum using the performance of the slowest component. Note that this is just one option for the model. The traces generated by the loop nest have enough information to produce a model that also accounts for the added latencies due to dependencies between components, though we leave its implementation to future work.

The format, architecture, and binding together specify the desired traces, allowing TeAAL to augment the loop nest to collect those traces. TeAAL provides a library of per-component models, which it adds calls to after the loop nest to translate the traces to action counts. If the corresponding Accelerger [45] specifications are provided, these action counts are passed to a power model to compute energy use.

Separately, the full cascade of Einsums, mappings, architectures, and bindings are used to determine whether individual Einsums are fused together, i.e., their computation is overlapped (see Section 3.1). TeAAL infers that Einsums can be fused together when three conditions are met:

- The Einsums use the same accelerator configuration.
- The temporal ranks in all loop orders before the first spatial rank are the same.
- All non-storage components are exclusively used by only one Einsum.

As a simple heuristic, it greedily fuses Einsums together into a single block, trying to minimize the number of Einsum blocks. Based on this fusion schedule, TeAAL translates the

outputs of the per-component models into execution time.

Evaluating on real data. TeAAL evaluates its model by running the specified kernel on real datasets. In doing so, it is able to fully capture the impact of the specific sparsity patterns of those tensors on the kernel’s performance, significantly improving TeAAL’s fidelity over that of analytical models. We quantitatively explore this phenomenon in Section 7 and Figure 9a.

5. ACCELERATOR SPECIFICATION

Sections 3-4 used OuterSPACE [31] as a running example. We now describe the Einsums and mapping specifications for three other, state-of-the-art accelerators relevant to our evaluation, shown in Figure 7. While preparing this work, we modeled a number of other accelerators whose details we omit for space, including Graphicionado [12] (Section 8), Eyeriss [7], and Tensaurus [40]. We also omit the format, architecture, and binding specifications for brevity.

Gamma [48]. Gamma (Figure 7a) is a row-wise Gustavson’s style accelerator that uses a tightly-pipelined multiply-merge style architecture to reduce partial output traffic and enable concordant traversal across both input and output tensors. In Gustavson’s dataflow, a row of A is combined and reduced with rows of B . Gamma distributes rows of A to each PE and, based on which values in each row are non-zero, the PE fetches a subset of the rows of B . This filtering is implemented using the `take(.)` operator (Section 3.1). After being fetched to each PE, the rows of B (which initially have rank order $[K, N]$) are sorted with hardware mergers to facilitate reduction over K . Similar to OuterSPACE, this is expressed as a rank swap: T has rank order $[M, K, N]$ and the rightmost (bottommost) rank in the loop order for the Einsum computing Z is K . Hence, the compiler inserts a rank swap on T , making its rank order $[M, N, K]$ in the context of the second Einsum. Unlike OuterSPACE, the two Einsums in the cascade are fused together, per the criteria described in Section 4.3.

ExTensor [14]. ExTensor (Figure 7b) employs a hybrid dataflow that is inner product-style at the innermost level. ExTensor’s two salient characteristics are the use of uniform shape-based partitioning (Section 2.3) and hierarchical intersection. Lines 14-23 describe this partitioning, while hierarchical intersection is accounted for implicitly due to fibertree semantics (Section 2.4). Note that our ExTensor specification includes details beyond the original paper from private correspondence with the authors about the actual design of the simulator used for evaluation.

SIGMA [35]. SIGMA (Figure 7c) is a deep-learning accelerator that uses occupancy-based partitioning to only distribute non-zero elements of the stationary matrix to PEs, reducing ineffectual compute. While SIGMA can be configured to support A and B -stationary dataflows, we only describe/evaluate the A -stationary dataflow here. SIGMA utilizes an Einsum cascade (Section 3.1), first removing all K -fibers (columns) of A that correspond to empty K -fibers (rows) in B (Line 8), then performing the multiplication (Line 9). We express the partitioning on Lines 18-20 using a combination of shape-based partitioning, flattening, and occupancy-based partitioning (Section 3.2.1). Finally, because all PEs work in parallel, the spatial dimension is $MK00$ (Line 29).


```

1 einsum:
2 declaration :
3 A: [K, M]
4 B: [K, N]
5 T: [K, M, N]
6 Z: [M, N]
7 expressions :
8 - T[k,m,n] = take(A[k,m], B[k,n], 1)
9 - Z[m,n] = T[k,m,n]*A[k,m]
10 mapping:
11 rank-order:
12 A: [M, K]
13 B: [K, N]
14 T: [M, K, N]
15 Z: [M, N]
16 partitioning :
17 T:
18 M: [uniform_occupancy(A.32)]
19 K: [uniform_occupancy(A.64)]
20 Z:
21 M: [uniform_occupancy(A.32)]
22 K: [uniform_occupancy(A.64)]
23 loop-order:
24 T: [M1, M0, K1, K0, N]
25 Z: [M1, M0, K1, N, K0]
26 spactime:
27 T:
28 space: [M0, K1]
29 time: [M1, K0, N]
30 Z:
31 space: [M0, K1]
32 time: [M1, N, K0]

```

(a) Gamma accelerator [48].

```

1 einsum:
2 declaration :
3 A: [K, M]
4 B: [K, N]
5 Z: [M, N]
6 expressions :
7 - Z[m,n] = A[k,m] * B[k,n]
8 mapping:
9 rank-order:
10 A: [K, M]
11 B: [K, N]
12 Z: [M, N]
13 partitioning :
14 Z:
15 K:
16 - uniform_shape(K1)
17 - uniform_shape(K0)
18 M:
19 - uniform_shape(M1)
20 - uniform_shape(M0)
21 N:
22 - uniform_shape(N1)
23 - uniform_shape(N0)
24 loop-order:
25 Z: [N2, K2, M2, M1, N1, K1, M0, N0, K0]
26 spactime:
27 Z:
28 space: [K1]
29 time: [N2, K2, M2, M1, N1, M0, N0, K0]

```

(b) ExTensor accelerator [14].

```

1 einsum:
2 declaration :
3 A: [K, M]
4 B: [K, N]
5 T: [K, M]
6 Z: [M, N]
7 expressions :
8 - T[k, m] = take(A[k, m], B[k, n], 0)
9 - Z[m, n] = T[k, m] * B[k, n]
10 mapping:
11 rank-order:
12 A: [K, M]
13 B: [K, N]
14 T: [K, M]
15 Z: [M, N]
16 partitioning :
17 Z:
18 K: [uniform_shape(128)]
19 (M, K0): [ flatten () ]
20 MK0: [uniform_occupancy(T.16384)]
21 loop-order:
22 T: [K, M, N]
23 Z: [K1, MK01, MK00, N]
24 spactime:
25 T:
26 space: []
27 time: [K, M, N]
28 Z:
29 space: [MK00]
30 time: [K1, MK01, N.coord]

```

(c) SIGMA accelerator [35].

Figure 7: State-of-the-art sparse tensor accelerators. `uniform_shape()/flatten()` are syntax for shape-based partitioning/flattening (Section 3.2.1), respectively.

Table 3: Tensor data set characteristics.

Matrix	Shape	NNZ	Domain
wiki-Vote (wi)	$8.3K \times 8.3K$	104K	elections
p2p-Gnutella31 (p2)	$63K \times 63K$	148K	file-sharing
ca-CondMat (ca)	$23K \times 23K$	187K	collab. net.
poisson3Da (po)	$14K \times 23K$	353K	fluid dynamics
email-Enron (em)	$37K \times 37K$	368K	email comms.
flickr (fl)	$0.82M \times 0.82M$	9.8M	site crawl graph
wikipedia-20070206 (wk)	$3.6M \times 3.6M$	42M	site link graph
soc-LiveJournal1 (lj)	$4.8M \times 4.8M$	69M	follower graph

Table 4: Hardware configs, chosen to match original publications.

ExTensor [14]	1 GHz clock speed, 128 PEs, 64 kB PE buffer per PE, 30 MB LLC, 68.256 GB/s memory bandwidth
Gamma [48]	1 GHz clock speed, 64-way merger per PE, 32 PEs, 3 MB Fiber-Cache, 16 64-bit HBM channels, 8 GB/s/channel
OuterSPACE [31]	1.5 GHz clock speed, 16 PEs per PT, 16 PTs, 16 kB L0 cache per PT, 4 kB L1 cache per 4 PTs, 16 64-bit HBM channels, 8000 MB/s/channel
SIGMA [35]	500 MHz clock speed, 128 PEs per FlexDPE, 128 FlexDPEs, 32 MB Data SRAM, 4 MB Bitmap SRAM, 960 GB/s SRAM bandwidth, 1024 GB/s HBM bandwidth
Graphiconado [12]	1 GHz clock speed, 8 streams, 64MB eDRAM, 68 GB/s memory bandwidth

6. EXPERIMENTAL SET-UP

This section describes the details of the experimental set-up used in Sections 7-8 to evaluate the performance characteristics of concrete accelerators.

Tensors. To evaluate the TeAAL models, we execute the models for the accelerators on a combination of randomly generated matrices with uniform sparsity and a set of matrices from SuiteSparse [9] and SNAP [22], described in Table 3.

Simulation Framework. We implement the four accelerators by writing TeAAL specifications for their Einsums, mappings, formats, architectures, and bindings. For each

accelerator, we use the hardware parameters given in Table 4. TeAAL uses Accelry [45] as a power model to convert the per-component action counts to an energy characterization.

Baselines. To validate our results, we normalize our performance estimates using the same baseline as the original papers that published the relevant accelerators. All accelerators’ “reported” statistics come either from published results or from private communication with the original authors. When possible, we also report Sparseloop [46] performance estimates using the *hypergeometric* sparsity distribution on both the inputs and outputs, estimated using the values in Table 3, and the hardware parameters in Table 4.

7. SIMULATOR VALIDATION

In this section, we describe a set of experiments used to validate TeAAL as an accurate cost model. Specifically, we compare memory traffic, performance, and power as reported by TeAAL to the numbers reported in the papers originally proposing each accelerator. We report all averages as arithmetic means, following the methodology presented in [19].

Memory Traffic. Figure 8 presents a comparison of the memory traffic of the TeAAL models of each of accelerators to the corresponding baseline. We use the first five tensors in Table 3 because the prior work evaluates these tensors. The takeaway is that we can reproduce each accelerator’s memory traffic with low error (on average, 3.8%).

Performance. Figure 9 presents a performance comparison of each TeAAL model against the reported numbers and Sparseloop [46]’s estimate, when possible. Figures 9a and 9b compare the speedup of ExTensor and Gamma, respectively, over Intel MKL according to the original simulator and the corresponding TeAAL model, on real-world matrices. TeAAL shows consistently low error rates for each (on



Figure 8: Comparison of the memory traffic reported by the original authors (left) and the TeAAL model (right) for ExTensor, Gamma, and OuterSPACE on 5 real-world tensors, discussed in Section 7. Traffic is normalized to the algorithmic minimum, and benchmark acronyms are defined in Table 3. Tensor names *A*, *B*, *T*, and *Z* correspond to the names defined in the Einsums in Figures 3 and 7. *PO* denotes the partial outputs (i.e. *Z* traffic that is not the final write of *Z*).

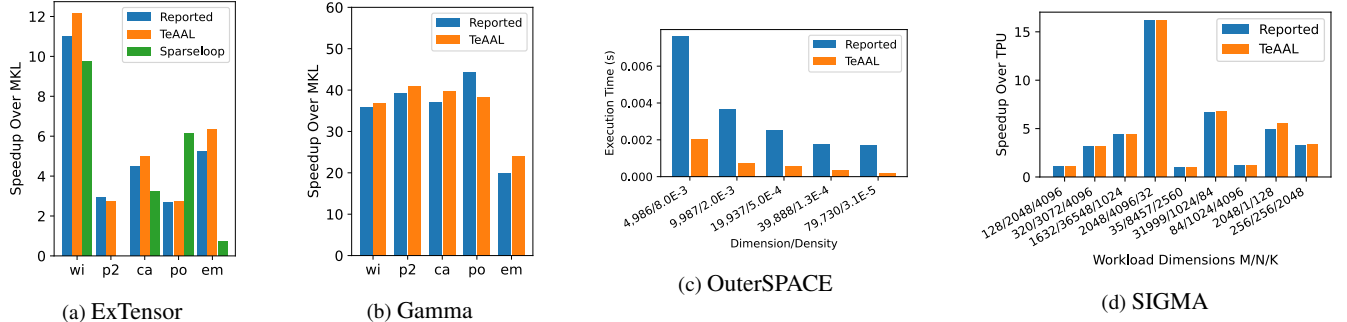


Figure 9: Validation of TeAAL-generated timing models against original publications, also discussed in Section 7. Benchmark acronyms in Table 3.

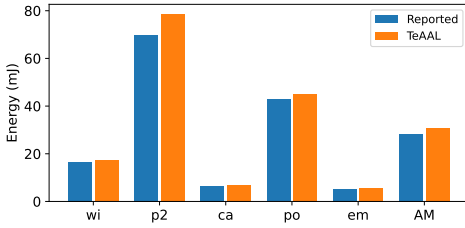


Figure 10: Validation of the ExTensor energy model, also discussed in Section 7. Benchmark acronyms can be found in Table 3.

```

1 # Processing Phase
2 - SO[d,s] = take(G[d,s], A0[s], 0)
3 - R[d] = SO[d,s]*A0[s]
4
5 # Apply Phase
6 - MP[v] = take(R[v], P0[v], 1)
7 - NP[v] = R[v]+MP[v]
8 - M[v] = NP[v]-MP[v]
9 - P0[v] = take(M[v], NP[v], 1)
10 - A1[v] = take(M[v], P0[v], 1)
11 - P1 = P0

```

(a) Graphiconado [12]

(b) Our Proposal

Figure 11: Einsum cascades for two vertex-centric programming accelerators. A specific algorithm manifests by redefining the multiplication and addition operators (e.g., for SSSP, to addition and minimum, respectively).

average, 10% and 6.4%, respectively). We perform an analogous evaluation for SIGMA in Figure 9d, relative to a Google Cloud TPU and over randomly generated matrices (where all matrices *A* and *B* had 80% and 10% sparsity, respectively). Here, we show an average error of only 2.5%.

We compare Sparseloop’s results to ours on ExTensor in Figure 9a.⁴ Sparseloop has an average error of 187%, which we attribute to its analytical sparsity distribution. We could not model p2 on Sparseloop because the tensor shape caused an integer overflow error.

Because we could not obtain the raw baseline used in the OuterSPACE paper, Figure 9c shows the performance of the original simulator and the TeAAL model on a number of uniformly sparse synthetic matrices. On average, our cost

model is about 80% faster than the original simulator, though the overall trend is consistent. In Figure 8c, we showed that TeAAL models OuterSPACE’s memory traffic with a $< 1.8\%$ error, so we suspect that the discrepancy in execution time comes from an undocumented (and, therefore, unmodeled) feature of the OuterSPACE PE microarchitecture.

Energy. Figure 10 compares TeAAL’s energy estimates to the reported baseline, showing consistently low error rates—on average, 7.8%. Since none of the other accelerators reported their per-component, per-action energy consumption characteristics, we were unable to validate the power model on those designs.

⁴We were unable to use Sparseloop to model Gamma/OuterSPACE (because it does not support cascades of Einsums) or SIGMA (because its occupancy-based partitioning is not sufficiently general).

8. IMPROVING GRAPHICIONADO

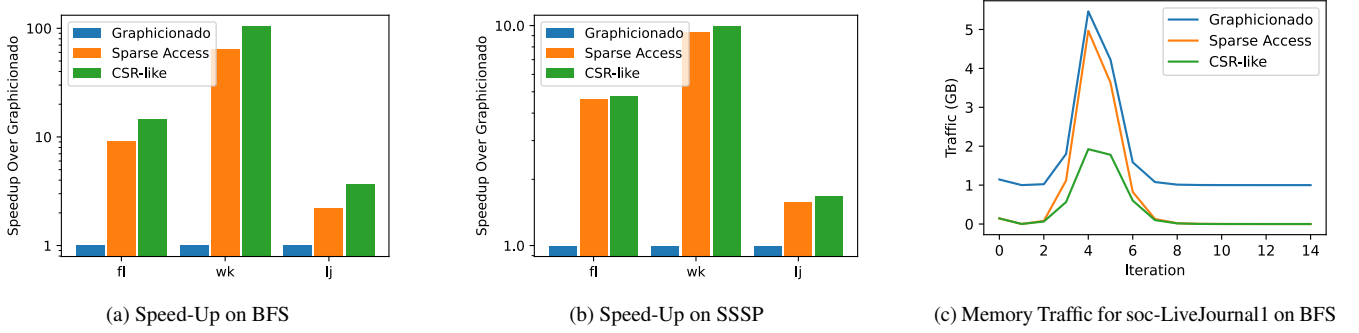


Figure 12: Comparison of Graphicionado to improved accelerators designed using TeAAL. All designs use the Graphicionado hardware parameters (Table 4).

In this section, we demonstrate both the generality of TeAAL as a tool for modeling a broader class of accelerators and the value of TeAAL when proposing and evaluating new designs. As an example, we model Graphicionado [12], which accelerates graph algorithms written in the vertex-centric programming paradigm, and use TeAAL to propose two optimizations.

Vertex-centric programming describes graph algorithms from the point of view of a single vertex. During each iteration, a vertex, if active, sends its property to all of its destination vertices. Then, the vertex, whether or not it is active, processes its incoming properties, reduces them to a single new value, and applies this value to its property [41]. For some algorithms (e.g., PageRank [30]), all vertices are active every iteration, while for other algorithms (e.g., breadth-first search (BFS)), only the vertices whose properties are updated are active in the next iteration [12]. In this evaluation, we will focus on the latter, more complex, class of algorithms.

Figure 11a shows a cascade of Einsums representing Graphicionado [12]. We omit the rest of the TeAAL specification for space. Graphicionado divides its evaluation into two stages. During the processing phase, the active vertices $A0$ are used to select the edges that need to be processed SO (Line 2), the weights of those edges are combined with the source vertex properties (Line 3), and reduced into R (implicit in Line 3). Then, during the apply phase, the vertex property $P0/P1$ is updated (Line 6) and the new set of active vertices $A1$ is created using a mask M of updated vertices (Lines 7-8). By redefining the multiplication and addition operators (e.g., for single source shortest path (SSSP), to addition and minimum, respectively), this represents a functionally correct implementation of a graph kernel written in the vertex-centric programming model. Through private correspondence with the authors of the Graphicionado paper, we found that all data, simulators, etc. used in this paper are proprietary, making it impossible for us to perform a similar analysis to Section 7. However, using TeAAL, we were able to profile Graphicionado ourselves and improve the design.

We optimized Graphicionado by adding new Einsums to the cascade to take advantage of the sparsity of R . This change requires a corresponding change in TeAAL’s *mapping*, *format*, and *binding* specifications. Figure 11b shows the updated cascade. Building an additional intermediate MP (Line 6), containing the values of $P0$ that can be modified, decreases the memory traffic incurred by $P0$ and the number

of apply operations the accelerator needs to perform. Filtering the writes to $P0$ with M (Line 9) also decreases the memory traffic. We further improve the design by changing the format of the graph from an edge-list representation to a CSR-like representation, which requires changing only the *format* specification. This format change eliminates unnecessary reloading of the source vertex ID and removes the loading of the edge weight for algorithms that do not use it (e.g., BFS).

We evaluate Graphicionado and our two new designs on a subset of the graphs and all sparse active vertex set algorithms evaluated in the original paper. Figure 12 shows the speedup achieved by each of our new designs (Sparse Access and CSR-like) over Graphicionado on BFS and SSSP. We note that our optimizations are cumulative, i.e. Sparse Access applies the cascade change to Graphicionado, and CSR-like applies the graph format change to Sparse Access. Figure 12a shows that our proposals enable an average of $26\times$ and $38\times$ improvement respectively over Graphicionado on BFS, while Figure 12b shows that our proposals enable an average of $4.1\times$ and $4.3\times$ improvement respectively over Graphicionado on SSSP. Figure 12c explains this improvement. The cascade optimization significantly reduces the memory traffic when the frontier is small, while the graph format optimization provides benefit when the frontier is large. Graphicionado was designed using the hypothesis that sequential memory accesses are better than random memory accesses, in part, because they use the entire buffer line’s worth of data. With TeAAL, we are able to show that, while random access of the properties cannot exploit spatial locality to the same extent, it significantly decreases traffic when the set of active vertices is small, improving performance.

9. RELATED WORK

The rise in machine learning and tensor algebra accelerators has been followed by an increase in tools that explore the accelerator design space and model performance and costs [2, 17, 20, 21, 25, 27, 32, 37, 46, 47]. Most frameworks solely support dense computations and target DNN applications [17, 21, 25, 32]. Table 5 compares frameworks that model architectures computing on sparse tensors. STONNE [27] is a cycle-level modeling framework for DNN accelerators. Like TeAAL, STONNE’s analysis is data-driven; however, the only sparse workload it supports is SpMSPM. CIN-P [2] is a mapper language that, when combined with an asymptotic

Table 5: Sparse tensor modeling frameworks.

	STONNE [26, 27]	CIN-P [2]	Sparseloop [46]	SAM [16]	TeAAL (this work)
Generic Kernels		✓	✓	✓	✓
Cascaded Einsums		✓		✓	✓
Index Expressions			✓		✓
Shape-Based Part.			✓	✓	✓
Occ.-Based Part.				✓	✓
Generic Flattening			✓	✓	✓
Rank Swizzling		✓			✓
Format Expressivity		✓	✓	✓	✓
Caches	✓				✓
Precise Data Set	✓			✓	✓
High Model Fidelity	✓				✓

cost model and autoscheduler, generates mappings that can then be compiled using TACO [20]. Since it uses asymptotic analysis, the mapper only considers loop order, loop fusion, and rank swizzling transformations. However, it does not consider partitioning and architectural features like caches or parallel units. Sparseloop [46], on the other hand, has a flexible hardware backend and takes as input a specification of the architecture, a statistical model of the data, sparse optimizations such as skip-based intersection [14], and a user-specified mapping. It returns estimates of performance and energy consumption. Unlike TeAAL, it does not support many of the mappings important to sparse computations, such as cascaded Einsums, caches, rank swizzling, and others. Additionally, CIN-P and Sparseloop analytically model the tensors' sparsity patterns. The data-driven nature of TeAAL enables cost estimates that better reflect the specific distribution of a given workload. The Sparse Abstract Machine (SAM) [16] targets an architecture consisting of hardware modules similar to those supported by TeAAL; however, it does not attempt to generate high-fidelity models of specific accelerator architectures.

10. CONCLUSION

This paper presents TeAAL: a language and compiler for describing and evaluating sparse tensor accelerators. The key contribution is to demonstrate how state-of-the-art sparse accelerators can be represented as cascades of mapped Einsums and content-preserving transformations on said Einsums' constituent tensors. From this observation, we propose the TeAAL language which enables designers to utilize and combine these concepts (for both the modeling of current and designing of new accelerators), and a compiler from this language to executable simulators that emulate fibertree operations (lowered onto concrete data representations and hardware units).

In the long term, we anticipate TeAAL will enable a more efficient accelerator design process supported by quantitative reasoning, while providing the architecture community with a common language for comparing and discussing designs. Also, while the current TeAAL backend generates performance/energy models, we think other backends (e.g., for generating hardware directly) are possible.

REFERENCES

- [1] [Online]. Available: <https://github.com/Fibertree-Project/fibertree>
- [2] P. Ahrens, F. Kjolstad, and S. P. Amarasinghe, "Autoscheduling for sparse tensor algebra with an asymptotic cost model," in *PLDI '22: 43rd ACM SIGPLAN International Conference on Programming Language Design and Implementation*, San Diego, CA, USA, June 13 - 17, 2022. ACM, 2022, pp. 269–285. [Online]. Available: <https://doi.org/10.1145/3519939.3523442>
- [3] H. M. Aktulga, A. Buluç, S. Williams, and C. Yang, "Optimizing sparse matrix-multiple vectors multiplication for nuclear configuration interaction calculations," in *IPDPS'14*, 2014.
- [4] J. Albericio, P. Judd, T. H. Hetherington, T. M. Aamodt, N. D. E. Jerger, and A. Moshovos, "Cnvlutin: Ineffective-neuron-free deep neural network computing," in *43rd ACM/IEEE Annual International Symposium on Computer Architecture, ISCA 2016, Seoul, South Korea, June 18-22, 2016*. IEEE Computer Society, 2016, pp. 1–13. [Online]. Available: <https://doi.org/10.1109/ISCA.2016.11>
- [5] A. Azad, A. Buluç, and J. Gilbert, "Parallel triangle counting and enumeration using matrix algebra," in *IPDPS'15 Workshop*, 2015.
- [6] T. Chen, T. Moreau, Z. Jiang, H. Shen, E. Q. Yan, L. Wang, Y. Hu, L. Ceze, C. Guestrin, and A. Krishnamurthy, "TVM: end-to-end optimization stack for deep learning," *CoRR*, vol. abs/1802.04799, 2018. [Online]. Available: <http://arxiv.org/abs/1802.04799>
- [7] Y.-H. Chen, J. Emer, and V. Sze, "Eyeriss: A spatial architecture for energy-efficient dataflow for convolutional neural networks," ser. *ISCA'16*.
- [8] S. Chou, F. Kjolstad, and S. Amarasinghe, "Format abstraction for sparse tensor algebra compilers," *Proc. ACM Program. Lang.*, vol. 2, no. OOPSLA, pp. 123:1–123:30, Oct. 2018. [Online]. Available: <https://doi.acm.org/10.1145/3276493>
- [9] T. A. Davis and Y. Hu, "The university of florida sparse matrix collection," *ACM Trans. Math. Softw.*, vol. 38, no. 1, dec 2011. [Online]. Available: <https://doi.org/10.1145/2049662.2049663>
- [10] S. Dongen, "Graph clustering by flow simulation," *PhD thesis, Center for Math and Computer Science (CWI)*, 05 2000.
- [11] A. Einstein, "The foundation of the general theory of relativity," *Annalen der Physik*, vol. 354, no. 7, pp. 769–822, Jan. 1916.
- [12] T. J. Ham, L. Wu, N. Sundaram, N. Satish, and M. Martonosi, "Graphiconado: A high-performance and energy-efficient accelerator for graph analytics," in *2016 49th Annual IEEE/ACM International Symposium on Microarchitecture (MICRO)*, 2016, pp. 1–13. [Online]. Available: <https://doi.org/10.1109/MICRO.2016.7783759>
- [13] S. Han, X. Liu, H. Mao, J. Pu, A. Pedram, M. A. Horowitz, and W. J. Dally, "Eie: efficient inference engine on compressed deep neural network," in *ISCA'16*.
- [14] K. Hegde, H. Asghari-Moghaddam, M. Pellauer, N. Crago, A. Jaleel, E. Solomonik, J. Emer, and C. W. Fletcher, "ExTensor: An Accelerator for Sparse Tensor Algebra," in *MICRO'19*.
- [15] K. Hegde, P.-A. Tsai, S. Huang, V. Chandra, A. Parashar, and C. W. Fletcher, "Mind Mappings: Enabling Efficient Algorithm-Accelerator Mapping Space Search," in *ASPLOS'21*.
- [16] O. Hsu, M. Strange, R. Sharma, J. Won, K. Olukotun, J. S. Emer, M. A. Horowitz, and F. Kjolstad, "The sparse abstract machine," in *Proceedings of the 28th ACM International Conference on Architectural Support for Programming Languages and Operating Systems, Volume 3, ASPLOS 2023, Vancouver, BC, Canada, March 25-29, 2023*, ser. ASPLOS 2023. ACM, 2023, pp. 710–726. [Online]. Available: <https://doi.org/10.1145/3582016.3582051>
- [17] Q. Huang, M. Kang, G. Dinh, T. Norell, A. Kalaiah, J. Demmel, J. Wawrzynek, and Y. S. Shao, "CoSA: Scheduling by constrained optimization for spatial accelerators," *2021 ACM/IEEE 48th Annual International Symposium on Computer Architecture (ISCA)*, pp. 554–566, 2021.
- [18] J. Hutter, M. Iannuzzi, F. Schiffmann, and J. VandeVondele, "CP2K: atomistic simulations of condensed matter systems," *WIREs Computational Molecular Science*, vol. 4, no. 1, pp. 15–25, 2014. [Online]. Available: <https://wires.onlinelibrary.wiley.com/doi/abs/10.1002/wcms.1159>
- [19] B. Jacob and T. N. Mudge, "Notes on calculating computer

- performance,” 1995. [Online]. Available: https://tmn.engin.umich.edu/wp-content/uploads/sites/353/2021/06/1995_Notes_on_calculating_computer_performance.pdf
- [20] F. Kjolstad, S. Kamil, S. Chou, D. Lugato, and S. Amarasinghe, “The tensor algebra compiler,” *Proceedings of the ACM on Programming Languages*, vol. 1, no. OOPSLA, pp. 77:1–77:29, Oct. 2017. [Online]. Available: <https://doi.org/10.1145/3133901>
 - [21] H. Kwon, M. Pellauer, and T. Krishna, “Maestro: An open-source infrastructure for modeling dataflows within deep learning accelerators,” *ArXiv*, vol. abs/1805.02566, 2018.
 - [22] J. Leskovec and A. Krevl, “SNAP Datasets: Stanford large network dataset collection,” <http://snap.stanford.edu/data>, Jun. 2014.
 - [23] M. Mahmoud, I. Edo, A. H. Zadeh, O. M. Awad, G. Pekhimenko, J. Albericio, and A. Moshovos, “TensorDash: Exploiting sparsity to accelerate deep neural network training,” in *53rd Annual IEEE/ACM International Symposium on Microarchitecture, MICRO 2020, Athens, Greece, October 17-21, 2020*. IEEE, 2020, pp. 781–795. [Online]. Available: <https://doi.org/10.1109/MICRO50266.2020.00069>
 - [24] T. Mattson, D. Bader, J. Berry, A. Buluc, J. Dongarra, C. Faloutsos, J. Feo, J. Gilbert, J. Gonzalez, B. Hendrickson, J. Kepner, C. Leiserson, A. Lumsdaine, D. Padua, S. Poole, S. Reinhardt, M. Stonebraker, S. Wallach, and A. Yoo, “Standards for graph algorithm primitives,” in *HPEC’13*, 2013.
 - [25] L. Mei, P. Houshmand, V. Jain, S. Giraldo, and M. Verhelst, “ZigZag: A memory-centric rapid DNN accelerator design space exploration framework,” 2020. [Online]. Available: <https://arxiv.org/abs/2007.11360>
 - [26] F. Muñoz-Martínez, R. Garg, M. Pellauer, J. L. Abellán, M. E. Acacio, and T. Krishna, “Flexagon: A multi-dataflow sparse-sparse matrix multiplication accelerator for efficient DNN processing,” in *Proceedings of the 28th ACM International Conference on Architectural Support for Programming Languages and Operating Systems, Volume 3, ASPLOS 2023, Vancouver, BC, Canada, March 25-29, 2023*. ACM, 2023, pp. 252–265. [Online]. Available: <https://doi.org/10.1145/3582016.3582069>
 - [27] F. Muñoz-Martínez, J. L. Abellán, M. E. Acacio, and T. Krishna, “STONNE: enabling cycle-level microarchitectural simulation for DNN inference accelerators,” *IEEE Computer Architecture Letters*, vol. 20, no. 2, pp. 122–125, 2021. [Online]. Available: <https://doi.org/10.1109/LCA.2021.3097253>
 - [28] Y. Nagasaka, S. Matsuoka, A. Azad, and A. Buluc, “Performance optimization, modeling and analysis of sparse matrix-matrix products on multi-core and many-core processors,” *Parallel Computing*, vol. 90, p. 102545, Dec. 2019. [Online]. Available: <https://doi.org/10.1016/j.parco.2019.102545>
 - [29] T. O. Odemuyiwa, H. Asghari-Moghaddam, M. Pellauer, K. Hegde, P.-A. Tsai, N. Crago, A. Jaleel, J. D. Owens, E. Solomonik, J. Emer, and C. Fletcher, “Accelerating sparse data orchestration via dynamic reflexive tiling,” in *Proceedings of the 28th ACM International Conference on Architectural Support for Programming Languages and Operating Systems*, ser. ASPLOS ’23, vol. 3, Mar. 2023. [Online]. Available: <https://doi.org/10.1145/3582016.3582064>
 - [30] L. Page, S. Brin, R. Motwani, and T. Winograd, “The pagerank citation ranking : Bringing order to the web,” in *The Web Conference*, 1999.
 - [31] S. Pal, J. Beaumont, D.-H. Park, A. Amarnath, S. Feng, C. Chakrabarti, H.-S. Kim, D. Blaauw, T. Mudge, and R. Dreslinski, “Outerspace: An outer product based sparse matrix multiplication accelerator,” 02 2018, pp. 724–736.
 - [32] A. Parashar, P. Raina, Y. S. Shao, Y.-H. Chen, V. A. Ying, A. Mukkara, R. Venkatesan, B. Khailany, S. W. Keckler, and J. Emer, “Timeloop: A systematic approach to dnn accelerator evaluation,” in *2019 IEEE International Symposium on Performance Analysis of Systems and Software (ISPASS)*, 2019, pp. 304–315.
 - [33] A. Parashar, M. Rhu, A. Mukkara, A. Puglielli, R. Venkatesan, B. Khailany, J. Emer, S. W. Keckler, and W. J. Dally, “Scnn: An accelerator for compressed-sparse convolutional neural networks,” in *ISCA’17*.
 - [34] M. Pellauer, Y. Shao, J. Clemons, N. Crago, K. Hegde, R. Venkatesan, S. Keckler, C. Fletcher, and J. Emer, “Buffets: An Efficient and Composable Storage Idiom for Explicit Decoupled Data Orchestration,” in *ASPLOS’19*.
 - [35] E. Qin, A. Samajdar, H. Kwon, V. Nadella, S. Srinivasan, D. Das, B. Kaul, and T. Krishna, “SIGMA: A sparse and irregular gemm accelerator with flexible interconnects for dnn training,” in *2020 IEEE International Symposium on High Performance Computer Architecture (HPCA)*, 2020, pp. 58–70.
 - [36] J. Ragan-Kelley, C. Barnes, A. Adams, S. Paris, F. Durand, and S. Amarasinghe, “Halide: A language and compiler for optimizing parallelism, locality, and recomputation in image processing pipelines,” *SIGPLAN Not.*, vol. 48, no. 6, p. 519–530, jun 2013. [Online]. Available: <https://doi.org/10.1145/2499370.2462176>
 - [37] R. Senanayake, C. Hong, Z. Wang, A. Wilson, S. Chou, S. Kamil, S. Amarasinghe, and F. Kjolstad, “A sparse iteration space transformation framework for sparse tensor algebra,” *Proc. ACM Program. Lang.*, vol. 4, no. OOPSLA, Nov. 2020. [Online]. Available: <https://doi.org/10.1145/3428226>
 - [38] E. Solomonik, M. Besta, F. Vella, and T. Hoefer, “Scaling betweenness centrality using communication-efficient sparse matrix multiplication,” in *Proceedings of the International Conference for High Performance Computing, Networking, Storage and Analysis*, 2017.
 - [39] N. Srivastava, H. Jin, J. Liu, D. Albonese, and Z. Zhang, “Matraport: A sparse-sparse matrix multiplication accelerator based on row-wise product,” in *2020 53rd Annual IEEE/ACM International Symposium on Microarchitecture (MICRO)*, 2020, pp. 766–780. [Online]. Available: <https://doi.org/10.1109/MICRO50266.2020.00068>
 - [40] N. Srivastava, H. Jin, S. Smith, H. Rong, D. Albonese, and Z. Zhang, “Tensaurus: A versatile accelerator for mixed sparse-dense tensor computations,” in *2020 IEEE International Symposium on High Performance Computer Architecture (HPCA)*, 2020, pp. 689–702. [Online]. Available: <https://doi.org/10.1109/HPCA47549.2020.00062>
 - [41] N. Sundaram, N. Satish, M. M. A. Patwary, S. R. Dulloor, M. J. Anderson, S. G. Vadlamudi, D. Das, and P. Dubey, “Graphmat: High performance graph analytics made productive,” *Proc. VLDB Endow.*, vol. 8, no. 11, p. 1214–1225, jul 2015. [Online]. Available: <https://doi.org/10.14778/2809974.2809983>
 - [42] V. Sze, Y. Chen, T. Yang, and J. S. Emer, *Efficient Processing of Deep Neural Networks*, ser. Synthesis Lectures on Computer Architecture. Morgan & Claypool Publishers, 2020. [Online]. Available: <https://doi.org/10.2200/S01004ED1V01Y202004CAC050>
 - [43] J. VandeVondele, U. Borštnik, and J. Hutter, “Linear scaling self-consistent field calculations with millions of atoms in the condensed phase,” *Journal of Chemical Theory and Computation*, vol. 8, no. 10, pp. 3565–3573, 2012, pMID: 26593003. [Online]. Available: <https://doi.org/10.1021/ct200897x>
 - [44] J. Wilhelm, P. Seewald, M. Del Ben, and J. Hutter, “Large-scale cubic-scaling random phase approximation correlation energy calculations using a gaussian basis,” *Journal of Chemical Theory and Computation*, vol. 12, no. 12, pp. 5851–5859, 2016, pMID: 27779863. [Online]. Available: <https://doi.org/10.1021/acs.jctc.6b00840>
 - [45] Y. N. Wu, J. S. Emer, and V. Sze, “Accelerger: An architecture-level energy estimation methodology for accelerator designs,” in *2019 IEEE/ACM International Conference on Computer-Aided Design (ICCAD)*, 2019, pp. 1–8. [Online]. Available: <https://doi.org/10.1109/ICCAD45719.2019.8942149>
 - [46] Y. N. Wu, P.-A. Tsai, A. Parashar, V. Sze, and J. S. Emer, “Sparseloop: An analytical approach to sparse tensor accelerator modeling,” *2022 55th IEEE/ACM International Symposium on Microarchitecture (MICRO)*, pp. 1377–1395, 2022. [Online]. Available: <https://doi.org/10.1109/MICRO56248.2022.00096>
 - [47] X. Yang, M. Gao, Q. Liu, J. Setter, J. Pu, A. Nayak, S. Bell, K. Cao, H. Ha, P. Raina, C. Kozyrakis, and M. Horowitz, “Interstellar: Using halide’s scheduling language to analyze dnn accelerators,” in *Proceedings of the Twenty-Fifth International Conference on Architectural Support for Programming Languages and Operating Systems*, ser. ASPLOS ’20. New York, NY, USA: Association for Computing Machinery, 2020, p. 369–383. [Online]. Available: <https://doi.org/10.1145/3373376.3378514>
 - [48] G. Zhang, N. Attaluri, J. S. Emer, and D. Sanchez, “Gamma: Leveraging gustavson’s algorithm to accelerate sparse matrix multiplication,” in *Proceedings of the 26th ACM International Conference on Architectural Support for Programming Languages and Operating Systems*, ser. ASPLOS 2021, 2021, pp. 687–701. [Online]. Available: <https://doi.org/10.1145/3445814.3446702>
 - [49] Z. Zhang, H. Wang, S. Han, and W. J. Dally, “Sparch: Efficient architecture for sparse matrix multiplication,” in *26th IEEE International Symposium on High Performance Computer Architecture*

(*HPCA*), 2020.